Article

Journal of the Brazilian Chemical Society

https://dx.doi.org/10.21577/0103-5053.20240003

J. Braz. Chem. Soc. **2024**, *35*, 6, e-20240003, 1-16

Versatile Applications of Cyanoacetic Acid in Organic Chemistry: Active Methylene Compound for the Knoevenagel Condensation and Organocatalyst for the Biginelli Reaction

Lucas L. Zanin,[a] David E. Q. Jimenez,*,[b] Gabriel D. S. Baia,[b] Victor H. Marinho,[b] Inana F. de Araujo,[b] Ryan D. S. Ramos,[c] Raimundo N. Soto,[d] Irlon M. Ferreira,[b] Pedro H. O. Santiago,[e] Javier Ellena[e] and André L. M. Porto[*,a]

[a]*Laboratório de Química Orgânica e Biocatálise, Instituto de Química de São Carlos, Universidade de São Paulo, Av. João Dagnone, 1100, Ed. Prof. Douglas Wagner Franco, Santa Angelina, 13563-120 São Carlos-SP, Brazil*

[b]*Laboratório de Biocatálise e Síntese Orgânica Aplicada, Universidade Federal do Amapá, Rod. Juscelino Kubitscheck, KM 02, S/N, Jardim Marco Zero, 68903-419 Macapá-AP, Brazil*

[c]*Laboratório de Modelagem e Química Computacional, Departamento de Ciências Biológicas e Saúde, Universidade Federal do Amapá, 68903-419 Macapá-AP, Brazil*

[d]*Laboratório de Artrópodes, Departamento de Biologia, Universidade Federal do Amapá, Rod. Juscelino Kubitscheck, KM 02, S/N, Jardim Marco Zero, 68903-419 Macapá-AP, Brazil*

[e]*Laboratório Multiusuário de Cristalografia Estrutural, Instituto de Física de São Carlos, Universidade de São Paulo, Av. Trabalhador São-Carlense, 400, Parque Arnold Schimidt, 13566-590 São Carlos-SP, Brazil*

The application of cyanoacetic acid as a catalyst for the Biginelli reaction and as an active methylene compound for the Knoevenagel condensation reaction was evaluated. Using cyanoacetic acid as a Bronsted acid catalyst, after a synthetic optimization process, it was possible to synthesize eight dihydropyrimidinones with good yields (80-99%) using ethanol as solvent. It is the first time, to our knowledge, that the use of cyanoacetic acid is reported in the synthesis of this class of compounds, which have a wide bioactive potential. Also, cyanoacetic acid was used as a reagent in the Knoevenagel condensation, through which polyfunctionalized olefins were obtained and can be used as building blocks for structurally complex molecules. By using KOH as catalyst, eleven Knoevenagel adducts were synthesized with good yields (65-97%), under microwave irradiation as heating source, in water. Moreover, Knoevenagel adducts containing halogenated substituents (F, Cl) showed potential larvicidal activity with lethal concentrations (LC_{50}) of 19.63, 33.84 μg mL^{-1} and LC_{90} of 27.46 and 48.16 μg mL^{-1}. This study showed the versatility of cyanoacetic acid as a catalyst for the synthesis of dihydropirimidinones, aldol compounds and presented the first study showing their larvicidal activity against *Aedes aegypti.*

Keywords: aldol condensation, green chemistry, microwave reaction, tricomponent reaction, biological assay, molecular docking

Introduction

The Knoevenagel and Biginelli reactions are very important protocols for organic chemistry. The Knoevenagel condensation is a type of aldol reaction widely used in the construction of new C–C bonds. Also, their products are excellent building blocks for structurally more complex molecules with relevant applications.[1,2]

The Biginelli synthesis is a three-component reaction with aldehydes, β-ketoesters or dicarbonyl compounds, and urea derivatives. Its products are known as dihydropyrimidinones (DHPMs) and are highly polyfunctionalized heterocyclic compounds that have important applications included in the field of medicinal chemistry with the discovery of the antitumoral properties

*e-mail: almporto@iqsc.usp.br; derteriom@unifap.br
Editor handled this article: Brenno A. D. Neto

of monastrol,[3] currently, they have a wide range of known biological properties, such as antihypertensive,[4] antioxidant,[5] anti-severe acute respiratory syndrome (anti-SARS),[6] anticonvulsant,[7] antitumoral,[8] antibacterial,[9] anti-inflammatory,[10] and among others.

An emerging research field involving the Biginelli reaction is polymer synthesis.[11-13] Polymers based on DHPM structures are polyfunctionalized, which makes the material susceptible to structural modifications after polymer formation through derivatization reactions. These processes can induce or increase properties of interest, such as light absorption or solubility. Mao *et al.*[14] synthesized a highly conjugated polymer based on the Biginelli reaction. The capacity of these materials was tested against ultra-violet (UV) light absorption, and they proved to be very effective, being able to insert these compounds, for example, in the field of development of novel types of sunscreens.

There are several synthetic methodologies for Knoevenagel condensation, which are employed with acidic and basic catalysts. Gilanizadeh and Zeynizadeh[15] developed a heterogeneous and reusable nanostructure catalyst, based on immobilization of Cu and Fe on silica as catalyst Lewis acid, aromatic aldehydes and malononitrile, to synthesize thirteen Knoevenagel adducts with excellent yields (90-97%) in times of 4-50 min, with the advantage of using water as a solvent under reflux conditions.

Likewise, the Biginelli reaction is a versatile protocol for the synthesis of organic compounds with complex structures. However, based on literature data, the vast majority of studies use Bronsted or Lewis acids as catalysts. Zanin and Porto[16] developed a heterogeneous catalyst for the Biginelli reaction. Using $HClO_4$-Al_2O_3, sixteen 3,4-dihydropyrimidin-2(1*H*)-ones/thiones were synthesized with good yields (80-94%) using aromatic aldehydes, ethyl acetoacetate, urea/thiourea and ethanol as solvent at 80 ºC for 1-3 h.

Another interesting reaction was studied by Jimenez *et al.*[17] using triethylamine in the synthesis of twenty-four Knoevenagel adducts with good yields (70-99%). The reactions were carried out in a microwave reactor, for 35 min, at 85 ºC and the solvents used were an aqueous solution of NaCl and EtOH (according to the activated methylene compound used malononitrile or methyl cyanoacetate).

Due to the various applications of DHPMs and Knoevenagel condensation, the research for new catalysts for these reactions remains relevant. Therefore, in this study, the versatility of cyanoacetic acid (CA) as an organocatalyst for the Biginelli reaction and a methylene active compound for the Knoevenagel reaction was evaluated.

Experimental

General methods

Fourier transform infrared (FTIR) spectra were recorded using Shimadzu IRAffinity-1 spectrometer model (Shimadzu, São Carlos, São Paulo, Brazil). Analyses were performed using compressed tablet disks prepared with KBr. The transmittance was expressed in cm^{-1} between 4000 and 450 cm^{-1}.

Nuclear magnetic resonance (NMR) spectra were recorded on an Agilent Technologies 500/54 Premium Shielded or Agilent Technologies 400/54 Premium Shielded spectrometer, with dimethyl sulfoxide (DMSO-d_6) or acetone-d_6 as solvent and tetramethylsilane (TMS) as the internal standard (Agilent Technologies, São Carlos, São Paulo, Brazil). The chemical shifts (δ) were expressed in parts *per* million (ppm) and referenced to the tetramethylsilane internal standard (TMS) signal and the deuterated solvent used DMSO-d_6 (δ_H 2.50, δ_C 39.52) and acetone-d_6 (δ_H 2.84 and 2.05, δ_C 206.26 and 29.8). For ^{1}H NMR spectra, the number of scans was 120 and for ^{13}C NMR was 881.

The reactions performed in a microwave (MW) reactor were performed using a Discover System from CEM Corporation at a 2.45 GHz frequency with maximal power output of about 200 W with internal magnetic stirring. For the reactions, the power of the microwave reactor used was 55 W (CEM Corporation, São Carlos, São Paulo, Brazil).

Melting points were measured in a Fisatom model 431 melting point apparatus in temperature interval of 25 to 300 ºC (Fisatom, São Carlos, São Paulo, Brazil).

The Biginelli reactions were monitored by a gas chromatograph-mass spectrometer (GC-MS-QP2010 Ultra) equipped with an auto-sampler injection AOC-20i (Shimadzu Corporation, São Carlos, São Paulo, Brazil). The detector used was of the electronic impact type (70 eV), scanning speed of 1.666, scan interval of 0.30 and fragments detected from 40 to 500 Da. Separations were performed on a fused silica capillary column (DB-5MS 5% phenyl-95%-dimethylpolysiloxane 30 m × 0.25 mm internal diameter, 0.25 mm film thickness) in a stream of helium of 0.95 mL min^{-1}. The injector temperature was 250 °C, the ion source was 200 °C, the interface was 270 °C and the split ratio was 5. The oven temperature program started at 70 °C, remaining for 2 min, with an increase of 20 ºC min^{-1} to 280 ºC, remaining for 8.54 min, resulting in a total time of 21 min.

The chromatographic yield of the optimization step of Biginelli reaction was performed by a Shimadzu

liquid chromatograph system (HPLC-PDA) equipped with LC-20AT pump, DGU-20A5 degasser, SIL-20AHT autosampler, SPD-M20A PDA detector, CTO-20A column oven, and CBM-20A controller, using a C18-phenomenex chromatographic column (250 mm × 4.6 mm, particle size of 5 μm) as the stationary phase and a mixture of deionized water (eluent A) and acetonitrile (eluent B) as the mobile phase, with linear gradient elution protocol: 15 to 100% of the eluent B in 40 min. The flow rate was 1.0 mL min^{-1} (Shimadzu Corporation, São Carlos, São Paulo, Brazil).

Chemical reagents

The following reactants: benzaldehyde (> 99%) **1a**, 4-bromobenzaldehyde (99%) **1b**, 4-chlorobenzaldehyde (97%) **1c**, 4-fluorobenzaldehyde (98%) **1d**, 4-methylbenzaldehyde (99%) **1e**, 4-nitrobenzaldehyde (99%) **1f**, 4-hydroxybenzaldehyde (98%) **1g**, 3,4,5-trimethoxybenzaldehyde (98%) **1h**, 4-methoxybenzaldehyde (97%) **1i**, 3-fluorobenzaldehyde (97%) **1j**, 2-fluorobenzaldehyde (97%) **1k**, 2-thiophenecarboxaldehyde (98%) **1l**, furfural (99%) **1m**, ethyl acetoacetate (99%) **2**, urea (99%) **3** and cyanoacetic acid (99%) **5** were purchased of Sigma-Aldrich (São Paulo, SP, Brazil) and used without further purification. The KOH (99%) and HCl (37%) were purchased of Synth (Diadema, SP, Brazil).

The deuterated solvents, acetone-d_6 (99%) and DMSO-d_6 (99%) were purchased from Cambridge Isotope Laboratories (Scielab, Rio de Janeiro, RJ, Brazil).

The thin layer chromatography (TLC) utilized was DC-Fertigfolien ALUGRAM® XTra SIL G/UV_{254} (layer: 0.20 mm silica 60 with fluorescent indicator UV_{254}) (São Carlos Química, São Carlos, São Paulo, Brazil).

The solvents (hexane, ethyl acetate, acetone, methanol and ethanol) were purchased from Aldrich, Synth, Merck and Vetec (São Paulo, SP, Brazil) and were used without further purification.

General procedure for the synthesis of DHPMs **4a-4h**

In a typical procedure, a mixture of aldehyde (0.5 mmol), urea (0.5 mmol), ethyl acetoacetate (1 mmol) and cyanoacetic acid (20 mol%) was placed in a round-bottom flask. The suspension was stirred at 80 ºC for 2 h. In the sequence, 200 μL of EtOH were added and the reaction proceeded for more 4 h. The reaction was monitored by TLC in a mixture of EtOAc-hexane 6:4. After completion of the reaction, the products were directly purified by flash column chromatography (silica gel 230-400 mesh) using the same mixture used in TLC.

All products were characterized by ^{1}H NMR, ^{13}C NMR, FTIR, GC-MS and melting point. The spectral and analytical data of the compounds **4a**-**4h** can be viewed in the Supplementary Information (SI) section.

General procedure for the synthesis of Knoevenagel adducts **6a**-**6e**, **6h**-**6m** using conventional heating

In a typical procedure, a mixture of aldehyde (1.0 mmol), cyanoacetic acid (1 mmol), KOH (20 mol%, 0.7 M) and water (5 mL) was placed in a round-bottom flask. The suspension was stirred at 75 ºC for 20 min. The reaction was monitored by TLC in a mixture of EtOAc-hexane 8:2. After completion of the reaction, it was added 1 mL of HCl (3 M) and the solution was stirred for 30 min. At the end of the reaction, extraction with ethyl acetate (3 × 25 mL) was carried out. The combined organic phases were concentrated under reduced pressure until total evaporation of the solvent. The obtained product was purified by column chromatography (silica gel 230-400 mesh) using the same mixture used in TLC.

All products were characterized by ^{1}H NMR, ^{13}C NMR, FTIR, GC-MS and melting point. The spectral and analytical data of the compounds **6a**-**6e**, **6h**-**6m** can be viewed in the SI section.

General procedure for the synthesis of Knoevenagel adducts **6a**-**6e**, **6h**-**6m** under microwave irradiation

A mixture of aldehyde (1 mmol), cyanoacetic acid (1 mmol), KOH (20 mol%, 0.7 M) and water (5 mL) was put in the MW reactor (50 W) for 20 min and stirred at 75 ºC. The reaction progress was monitored by TLC in a mixture of EtOAc-hexane 8:2. After completion of the reaction, it was added 1 mL of HCl (3 M) and the solution was stirred for 30 min. At the end of the reaction, extraction with ethyl acetate (3 × 25 mL) was carried out. The combined organic phases were concentrated under reduced pressure until total evaporation of the solvent. The obtained product was purified by column chromatography (silica gel 230 400 mesh) using the same mixture used in TLC.

All products were characterized by ^{1}H NMR, ^{13}C NMR, FTIR and melting point. The spectral and analytical data of the compounds **6a**-**6m** can be viewed in the SI section.

Crystallization of Knoevenagel adducts **6a**, **6h**, **6l** and **6m**

All the crystallization of the Knoevenagel adducts followed the same protocols. First, 20 mg of each compound were put in a vial of 10 mL and were dissolved in 10 mL of acetone and methanol (1:1) and stirred at soft heating conditions (50 °C) for 5 min or until complete

solubilization. Then, the crystallization batches were allowed to cool down slowly and covered the vial with Parafilm® for slow evaporation of the solvent. All these systems were maintained at room temperature until the appearance of suitable single-crystals, which occurred within 1-2 days.

Single crystal structure determination of Knoevenagel adducts **6a**, **6h**, **6l** and **6m**

The single crystal X-ray diffraction measurements for **6a**, **6h**, **6l** and **6m** were performed at 293 K on a Rigaku XtaLAB mini (ROW) diffractometer with graphite monochromated Mo Kα radiation (0.71073 Å). Cell refinements were performed using the CrysAlisPro software.[18] Using Olex2,[19] the structures were solved by intrinsic phasing method SHELXT-14,[20] and refined by full-matrix least squares on F2 using the SHELXL.[21] The non-hydrogen atoms were refined anisotropically. Then, all hydrogen atoms were located from electron-density difference maps and were positioned geometrically and refined using the riding model [Uiso(H) = 1.2Ueq or 1.5Ueq]. The Olex2 was also used for analysis and visualization of the structures, and for graphic material preparation. The X-ray diffraction data and refinement parameters obtained for the elucidated crystal structures are summarized in Table 1. The Crystallographic Information File (CIF) of Knoevenagel adduct derivatives **6a**, **6h**, **6l** and **6m** were deposited in the Cambridge Structural Data Base[22] under the Cambridge Crystallographic Data Centre (CCDC) numbers 2298597, 2298598, 2298599 and 2298600, respectively.

Larvicidal bioassay

The larvae of *Aedes aegypti* and Rokeffeller colony were from the Arthropod Laboratory of the Federal University of Amapá (ARTHROLAB); all larvae used were in the 3rd stage. They were kept in standard weather conditions with a temperature of 25 ± 2 °C and relative humidity of

Table 1. Crystallographic data and refinement parameters for **6a**, **6h**, **6l** and **6m**

	6a	**6h**	**6l**	**6m**
Chemical formula	$C_{10}H_7NO_2$	$C_{13}H_{13}NO_5$	$C_8H_5NO_2S$	$C_8H_5NO_3$
M / (g mol^{-1})	173.17	263.24	179.19	163.13
Crystal system	triclinic	triclinic	triclinic	monoclinic
Space group	P-1	P-1	P-1	$P2_1/c$
a / Å	5.7567(8)	3.9668(7)	5.6375(9)	3.7917(7)
b / Å	8.5963(14)	10.5091(18)	8.8841(13)	15.2568(16)
c / Å	9.4356(15)	18.313(3)	8.9905(16)	12.653(2)
α / degree	64.738(16)	94.155(12)	117.344(16)	90
β / degree	83.045(12)	95.513(13)	97.741(14)	91.847(15)
γ / degree	87.021(12)	90.713(15)	90.683(12)	90
V / Å^3	419.17(12)	757.7(2)	394.93(12)	731.6(2)
Z	2	2	2	4
Density / (g cm^{-3})	1.372	1.154	1.507	1.481
θ_{min} / degree	5.24	5.71	5.18	5.34
θ_{max} / degree	51.36	50.69	54.20	51.36
μ / mm^{-1}	0.097	0.09	0.360	0.116
Absorption correction	multi-scan	multi-scan	multi-scan	multi-scan
Max./min. transmission	1.000/0.852	1.000/0.584	1.000/0.773	1.000/0.780
Measured reflections	2352	4112	2488	3895
Independent reflections / R_{int}	1578/0.0128	2763/0.0432	1747/0.0179	1348/0.0456
Refined parameters	119	178	110	110
R_1 [I ≥ 2σ(I)]	0.0416	0.0984	0.0481	0.0672
wR_2	0.1129	0.3028	0.1241	0.2067
GooF	1.074	1.217	1.085	1.111
Larg.t diff. peak and hole / (e Å^{-3})	0.19/–0.23	0.32/–0.36	0.30/–0.26	0.38/–0.36

M: molar mass; a-c and α-γ: unit cell parameters; V: volume; Z: formula unit *per* unit cell; R_{int}: internal R-value; R1: R-value; wR2: R-value for F2; GooF: goodness of fit; μ: micrometer.

75 ± 5% and photoperiod of 12 h according to the World Health Organization (WHO).[23]

Compounds **6a**-**6e**, **6h**-**6m** were prepared in different concentrations (75, 50, 25, 15 and 7.5 μg mL^{-1}) solubilized in DMSO (1%) from stock solution of 900 μg mL^{-1}. In each bioassay was used 10 larvae in controlled conditions (25 ± 2 °C). The distilled water and DMSO (1%) were used with negative controls. All assays were performed in quintuplicate.[24]

For larvicidal activity the lethal concentrations (LC_{50} and LC_{90}) were determined after 24 and 48 h of incubation and calculated using Probit analysis with Minitab 19 statistical software.[25]

Design and optimization of Knoevenagel adducts

Energy minimization for all structures was obtained through Density Functional Theory (DFT) calculations, B3LYP method, together with the 6-31G(d,p) base sets, using Gaussian 09 software to obtain bioactive poses.[26-28]

Molecular docking simulation

After obtaining bioactive poses, the compounds **6a**-**6e** and **6h**-**6m** were selected for molecular docking simulations, in order to evaluate the score of the binding free energy function (ΔG), as well as the analysis of conformations, interaction mode and binding affinity with the selected receptor.

Selection of the inhibitor structure

Crystallographic structure of juvenile hormone complexed with methyl (2*E*,6*E*)-9-[(2*R*)-3,3-dimethyloxiran-2-yl]-3,7-dimethylnona-2,6-dienoate ligand (JHIII), was downloaded with the PDB ID code 5V13 with a resolution of 1.87 Å. JHIII was used as a control ligand in the molecular docking study. The structure of juvenile hormone can be seen in Figure 1.

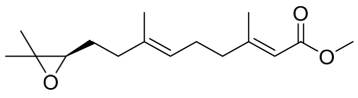

Figure 1. Structures of methyl(2*E*,6*E*)-9-[(2*R*)-3,3-dimethyloxiran-2-yl]-3,7-dimethylnona-2,6-dienoate (JHIII).

Molecular docking study

Ligands and protein structure used in molecular docking were prepared using Discovery Studio 5.0 software.[29] Validation of docking protocols in the molecular target (PDB ID 5V13) was performed by overlay the ligand crystal structure on the best docking pose for root mean square deviation (RMSD) calculation. In the juvenile hormone (*Aedes aegypti* organism) docking study, specific complexed ligands were used in AutoDock 4.2[30]/ Vina 1.1.2[31] via graphical interface PyRx 0.8.30.[32]

The x, y and z coordinates were determined according to the binding site on the receptor. The coordinates used for the grid center and dimensions can be seen in Table 2.

Characterization of the DHPMS **4a**-**4h**

Ethyl 6-methyl-2-oxo-4-phenyl-1,2,3,4-tetrahydropyrimidine-5-carboxylate (**4a**)

$C_{14}H_{16}N_2O_3$, 260.11 g mol^{-1}; 94% yield; white solid; mp 192-195 ºC; FTIR ν_{max} / cm^{-1} 3240, 3113, 2935, 1730, 1695, 1650, 1467, 1419, 1311, 1285, 1222, 1095, 1027, 780, 696; ^{1}H NMR (500 MHz, DMSO-d_6) δ 9.17 (s, 1H, NH), 7.72 (s, 1H, NH), 7.32 (m, 2H), 7.24 (m, 3H), 5.15 (d, *J* 3 Hz, 1H), 3.98 (q, *J* 7 Hz, 2H), 2.25 (s, 3H), 1.09 (t, *J* 7 Hz, 3H); ^{13}C NMR (125 MHz, DMSO-d_6) δ 165.3, 152.1, 148.3, 144.9, 128.4, 127.2, 126.2, 99.2, 59.2, 54.0, 17.7, 14.0; MS (70 eV) *m/z*, 183 (100%), 231 (79%), 155 (39%), 187 (36%), 137 (30%), 214 (29%), 260 (26%), 215 (14%).

Ethyl 4-(4-bromophenyl)-6-methyl-2-oxo-1,2,3,4-tetrahydropyrimidine-5-carboxylate (**4b**)

$C_{14}H_{15}BrN_2O_3$, 339.19 g mol^{-1}; 84% yield; white solid; mp 210-213 ºC; FTIR ν_{max} / cm^{-1} 3230, 3106, 2978, 2926, 1701, 1643, 1595, 1499, 1460, 1325, 1287, 1220, 1153, 1085, 787, 604; ^{1}H NMR (500 MHz, DMSO-d_6) δ 9.24 (s, 1H, NH), 7.77 (s, 1H, NH), 7.53 (d, *J* 8 Hz, 2H), 7.18 (d, *J* 8 Hz, 2H), 5.12 (d, *J* 3 Hz, 1H), 3.98 (q, *J* 7 Hz, 2H), 2.24 (s, 3H), 1.09 (t, *J* 7 Hz, 3H); ^{13}C NMR (125 MHz, DMSO-d_6) δ 165.2, 151.9, 148.7, 144.2, 131.3, 128.6, 120.3, 98.8, 59.3, 53.5, 17.8, 14.1; MS (70 eV) *m/z*, 183 (100%), 155 (43%), 309 (43%), 311 (40%), 137 (35%), 265 (25%), 267 (21%), 184 (13%).

Table 2. Data from protocols used here for molecular docking validation

Enzyme	Ligand	Grid center	Grid size / points
Juvenile hormone (PDB ID 5V13)	methyl (2*E*,6*E*)-9-[(2*R*)-3,3-dimethyloxiran-2-yl]-3,7-dimethylnona-2,6-dienoate	X = 239.509 Y = –26.714 Z = 353.130	36 x 24 y 24 z

Ethyl 4-(4-chlorophenyl)-6-methyl-2-oxo-1,2,3,4-tetrahydropyrimidine-5-carboxylate (**4c**)

$C_{14}H_{15}ClN_2O_3$, 294.08 g mol^{-1}; 98% yield; white solid; mp 204-206 ºC; FTIR ν_{max} / cm^{-1} 3234, 3114, 2978, 2954, 2929, 1701, 1639, 1487, 1460, 1421, 1323, 1288, 1222, 1093, 1011, 778, 680, 598; ^{1}H NMR (500 MHz, DMSO-d_6) δ 9.24 (s, 1H, NH), 7.76 (s, 1H, NH), 7.39 (d, *J* 8 Hz, 2H), 7.25 (d, *J* 8 Hz, 2H), 5.14 (d, *J* 3 Hz, 1H), 3.98 (q, *J* 7 Hz, 2H), 2.25 (s, 3H), 1.09 (t, *J* 7 Hz, 3H); ^{13}C NMR (125 MHz, DMSO-d_6) δ 165.2, 151.9, 148.7, 143.8, 131.8, 128.4, 128.2, 98.8, 59.3, 53.4, 17.8, 14.1; MS (70 eV) *m/z*, 183 (100%), 265 (84%), 155 (50%), 137 (44%), 221 (43%), 267 (28%), 42 (19%), 294 (17%).

Ethyl 4-(4-fluorophenyl)-6-methyl-2-oxo-1,2,3,4-tetrahydropyrimidine-5-carboxylate (**4d**)

$C_{14}H_{15}FN_2O_3$, 278.10 g mol^{-1}; 86% yield; white solid; mp 170-172 °C ; FTIR ν_{max} / cm^{-1} 3232, 3105, 2974, 2924, 1706, 1639, 1592, 1499, 1458, 1324, 1287, 1215, 1153, 1086, 1003, 781, 595; ^{1}H NMR (500 MHz, DMSO-d_6) δ 9.20 (s, 1H, NH), 7.73 (s, 1H, NH), 7.26 (m, 2H), 7.14 (m, 2H), 5.15 (d, *J* 3 Hz, 1H), 3.98 (qd, *J* 7 and 2 Hz, 2H), 2.25 (s, 3H), 1.09 (t, *J* 7 Hz, 3H); ^{13}C NMR (125 MHz, DMSO-d_6) δ 165.2, 161.3 (d, $^1J_{CF}$ 243 Hz), 152.0, 148.5, 141.1 (d, $^4J_{CF}$ 3 Hz), 128.2 (d, $^3J_{CF}$ 8 Hz), 115.1 (d, $^2J_{CF}$ 21 Hz), 99.1, 59.2, 53.3, 17.7, 14.1; MS (70 eV) *m/z*, 249 (100%), 183 (60%), 205 (44%), 155 (31%), 278 (25%), 137 (23%), 250 (15%), 42 (14%).

Ethyl 6-methyl-2-oxo-4-(*p*-tolyl)-1,2,3,4-tetrahydropyrimidine-5-carboxylate (**4e**)

$C_{15}H_{18}N_2O_3$, 274.13 g mol^{-1}; 96% yield; white solid; mp 205-207 ºC; FTIR ν_{max} / cm^{-1} 3238, 3103, 2917, 1726, 1692, 1644, 1456, 1417, 1284, 1224, 1078, 777; ^{1}H NMR (500 MHz, DMSO-d_6) δ 9.14 (s, 1H, NH), 7.67 (s, 1H, NH), 7.11 (s, 4H), 5.10 (d, *J* 3 Hz, 1H), 3.98 (q, *J* 7 Hz, 2H), 2.26 (s, 3H), 2.24 (s, 3H), 1.10 (t, *J* 7 Hz, 3H); ^{13}C NMR (125 MHz, DMSO-d_6) δ 165.3, 152.2, 148.1, 141.9, 136.3, 129.1, 128.9, 126.1, 99.4, 59.1, 53.6, 20.6, 17.8, 14.1; MS (70 eV) *m/z*, 183 (100%), 245 (88%), 201 (56%), 155 (51%), 137 (46%), 228 (28%), 274 (22%), 115 (16%).

Ethyl 6-methyl-4-(4-nitrophenyl)-2-oxo-1,2,3,4-tetrahydropyrimidine-5-carboxylate (**4f**)

$C_{14}H_{15}N_3O_5$, 305.10 g mol^{-1}; 80% yield; light yellow solid; mp 201-203 ºC; FTIR ν_{max} / cm^{-1} 3233, 3110, 2949, 1732, 1698, 1641, 1521, 1463, 1347, 1285, 1215, 1082, 1017, 851, 777, 694, 657; ^{1}H NMR (500 MHz, DMSO-d_6) δ 9.34 (s, 1H, NH), 8.21 (d, *J* 8 Hz, 2H), 7.88 (s, 1H, NH), 7.51 (d, *J* 8 Hz, 2H), 5.28 (s, 1H), 3.99 (q, *J* 7 Hz, 2H), 2.27 (s, 3H), 1.09 (t, *J* 7 Hz, 3H); ^{13}C NMR (125 MHz, DMSO-d_6) δ 165.0, 152.0, 151.8, 149.4, 146.7, 127.7, 123.8, 98.2, 59.4, 53.7, 17.9, 14.0; MS (70 eV) *m/z*, 183 (100%), 276 (77%), 155 (67%), 137 (60%), 42 (27%), 186 (23%), 232 (22%), 230 (16%).

Ethyl 4-(4-hydroxyphenyl)-6-methyl-2-oxo-1,2,3,4-tetrahydropyrimidine-5-carboxylate (**4g**)

$C_{14}H_{16}N_2O_4$, 276.11 g mol^{-1}; 81% yield; yellow solid; mp 218-220 ºC ; FTIR ν_{max} / cm^{-1} 3275, 2918, 1683, 1630, 1511, 1442, 1368, 1311, 1266, 1216, 1089, 1016, 832, 750, 651; ^{1}H NMR (500 MHz, DMSO-d_6) δ 9.31 (s, 1H, OH), 9.10 (s, 1H, NH), 7.60 (s, 1H, NH), 7.02 (d, *J* 8 Hz, 2H), 6.68 (d, *J* 8 Hz, 2H), 5.04 (d, *J* 3 Hz, 1H), 3.97 (q, *J* 7 Hz, 2H), 2.23 (s, 3H), 1.10 (t, *J* 7 Hz, 3H); ^{13}C NMR (125 MHz, DMSO-d_6) δ 165.4, 156.5, 152.2, 147.8, 135.5, 127.4, 115.0, 99.7, 59.1, 53.4, 17.7, 14.1; MS (70 eV) *m/z*, 247 (100%), 203 (61%), 183 (58%), 155 (55%), 137 (49%), 42 (27%), 110 (23%), 276 (19%).

Ethyl 6-methyl-2-oxo-4-(3,4,5-trimethoxyphenyl)-1,2,3,4-tetrahydropyrimidine-5-carboxylate (**4h**)

$C_{17}H_{22}N_2O_6$, 350.15 g mol^{-1}; 90% yield; light yellow solid; mp 176-178 ºC; FTIR ν_{max} / cm^{-1} 3226, 3095, 2923, 2831, 1716, 1707, 1647, 1586, 1508, 1465, 1421, 1330, 1283, 1244, 1222, 1122, 1088, 1001, 793, 771, 702, 633; ^{1}H NMR (500 MHz, DMSO-d_6) δ 9.19 (s, 1H, NH), 7.71 (s, 1H, NH), 6.52 (s, 2H), 5.11 (d, *J* 3 Hz, 1H), 4.02 (m, 2H), 3.72 (s, 6H), 3.63 (s, 3H), 2.25 (s, 3H), 1.13 (t, *J* 7 Hz, 3H); ^{13}C NMR (125 MHz, DMSO-d_6) δ 165.4, 152.8, 152.3, 148.5, 140.5, 136.8, 103.4, 99.0, 60.0, 59.2, 55.8, 53.9, 17.8, 14.2; MS (70 eV) *m/z*, 350 (100%), 321 (68%), 183 (57%), 277 (53%), 304 (50%), 303 (36%), 155 (34%), 319 (33%).

Characterization of the Knoevenagel adducts **6a**-**6e** and **6h**-**6m**

(*E*)-2-Cyano-3-phenylacrylic acid (**6a**)

$C_{10}H_7NO_2$, 173.05 g mol^{-1}; 71% yield; white crystal, mp 179-182 ºC; FTIR ν_{max} / cm^{-1} 3460, 2963, 2928, 2228, 1700, 1605, 1589, 1492, 1412, 1284, 1201, 1185, 1092, 1012, 828, 787, 725; ^{1}H NMR (500 MHz, DMSO-d_6) δ 8.34 (s, 1H), 8.04-8.01 (m, 2H), 7.64-7.56 (m, 3H); ^{13}C NMR (125 MHz, DMSO-d_6) δ 163.7, 154.9, 133.6, 132.0, 131.1, 131.1, 129.7, 116.5, 104.3.

(*E*)-3-(4-Bromophenyl)-2-cyanoacrylic acid (**6b**)

$C_{10}H_6NBrO_2$, 250.96 g mol^{-1}; 82% yield; yellow solid, mp 179-182 ºC; FTIR ν_{max} / cm^{-1} 3192, 3087, 2924, 2228, 1706, 1605, 1529, 1490, 1406, 1282, 1208, 1187, 1076, 1009, 824; ^{1}H NMR (500 MHz, DMSO-d_6) δ 8.31 (s, 1H),

7.96-7.94 (d, *J* 8.0 Hz, 2H), 7.81-7.78 (d, *J* 8.0 Hz, 2H); ^{13}C NMR (125 MHz, DMSO-d_6) δ 163.5, 153.4, 132.8, 132.7, 131.3, 127.2, 116.4, 105.3.

(*E*)-3-(4-Chlorophenyl)-2-cyanoacrylic acid (**6c**)

$C_{10}H_6NClO_2$, 207.01 g mol^{-1}; 85% yield; yellow solid, mp 192-194 ºC; FTIR ν_{max} / cm^{-1} 3448, 3027, 2904, 2842, 2228, 1702, 1690, 1492, 1589, 1492, 1422, 1280, 1212, 1191, 1092, 1014, 828; ^{1}H NMR (400 MHz, DMSO-d_6) δ 8.32 (s, 1H), 8.04-8.00 (d, *J* 8.0 Hz, 2H), 7.66-7.63 (d, *J* 8.0 Hz, 2H); ^{13}C NMR (100 MHz, DMSO-d_6) δ 163.5, 153.4, 138.1, 132.7, 131.6, 130.9, 129.9, 129.2, 116.4, 105.0.

(*E*)-2-Cyano-3-(4-fluorophenyl)acrylic acid (**6d**)

$C_{10}H_6NFO_2$, 191.04 g mol^{-1}; 75% yield; yellow solid, mp 187-189 ºC; FTIR ν_{max} / cm^{-1} 3345, 2926, 2246, 1706, 1605, 1583, 1489, 1422, 1408, 1278, 1204, 1074, 1010, 822; ^{1}H NMR (400 MHz, DMSO-d_6) δ 8.34 (s, 1H), 8.13-8.09 (dd, *J* 8.7 and 5.6 Hz, 2H), 7.45-7.41 (t, *J* 8.8 Hz, 2H); ^{13}C NMR (125 MHz, DMSO-d_6) δ 168.9, 163.7, 153.6, 134.0, 133.9, 128.7, 117.1, 116.9, 116.5, 103.9.

(*E*)-2-Cyano-3-(*p*-tolyl)acrylic acid (**6e**)

$C_{11}H_9NO_2$, 187.06 g mol^{-1}; 83% yield; yellow solid, mp 187-189 ºC; FTIR ν_{max} / cm^{-1} 3116, 2914, 2224, 1688, 1581, 1410, 1282, 1218, 1057, 944, 861, 740; ^{1}H NMR (500 MHz, DMSO-d_6) δ 8.27 (s, 1H), 7.94 (d, *J* 8.0 Hz, 2H), 7.39 (d, *J* 8.0 Hz, 2H), 2.38 (s, 3H); ^{13}C NMR (125 MHz, DMSO-d_6) δ 169.0, 164.0, 154.6, 144.4, 131.2, 130.4, 129.3, 116.8, 21.8.

(*E*)-2-Cyano-3-(3,4,5-trimethoxyphenyl)acrylic acid (**6h**)

$C_{13}H_{13}NO_5$, 263.08 g mol^{-1}; 78% yield; yellow solid, mp 206-208 ºC; FTIR ν_{max} / cm^{-1} 3497, 3005, 2945, 2842, 2222, 1717, 1692, 1577, 1502, 1454, 1422, 1329, 1251, 1158, 1123, 895, 835; ^{1}H NMR (500 MHz, DMSO-d_6) δ 8.28 (s, 1H), 7.49 (s, 2H), 3.83 (s, 6H), 3.78 (s, 3H); ^{13}C NMR (125 MHz, DMSO-d_6) δ 163.9, 154.8, 153.3, 142.2, 127.1, 116.9, 109.1, 107.2, 102.5, 60.8, 56.5, 56.5.

(*E*)-2-Cyano-3-(4-methoxyphenyl)acrylic acid (**6i**)

$C_{11}H_9NO_3$, 203.06 g mol^{-1}; 78% yield; yellow solid, mp 199-201 ºC; FTIR ν_{max} / cm^{-1} 3023, 2980, 2930, 2843, 2224, 1673, 1587, 1556, 1511, 1428, 1294, 1261, 1230, 1175, 1020, 938, 833, 810, 767, 732; ^{1}H NMR (400 MHz, DMSO-d_6) δ 8.21 (s, 1H), 8.03 (d, *J* 8.8, 2H), 7.11 (d, *J* 8.8 Hz, 2H), 3.83 (s, 1H); ^{13}C NMR (100 MHz, DMSO-d_6) δ 164.3, 163.6, 154.0, 133.6, 124.6, 117.3, 115.3, 100.1, 56.1.

(*E*)-2-Cyano-3-(3-fluorophenyl)acrylic acid (**6j**)

$C_{10}H_6NFO_2$, 191.04 g mol^{-1}; 68% yield; yellow solid, mp 174-177 ºC; FTIR ν_{max} / cm^{-1} 3404, 3332, 3190, 3005, 2943, 2840, 2215, 1688, 1581, 1502, 1461, 1422, 1389, 1327, 1241, 1121, 995, 835, 723, 629; ^{1}H NMR (400 MHz, acetone-d_6) δ 8.35 (s, 1H), 7.93-7.86 (m, 2H), 7.69-7.63 (td, *J* 8.1 and 5.9 Hz, 1H), 7.43 (tdd, *J* 8.5, 2.6 and 0.9 Hz, 1H); ^{13}C NMR (100 MHz, acetone-d_6) δ 163.9, 162.2, 161.4, 153.1, 153.1, 134.0, 133.9, 131.3, 131.2, 127.0, 127.0, 119.9, 119.8, 119.7, 119.6, 116.8, 116.6, 115.2, 105.2.

(*E*)-2-Cyano-3-(2-fluorophenyl)acrylic acid (**6k**)

$C_{10}H_6NFO_2$, 191.04 g mol^{-1}; 65% yield; yellow solid, mp 169-172 ºC; FTIR ν_{max} / cm^{-1} 3155, 3130, 3040, 2918, 2220, 1671, 1597, 1533, 1427, 1399, 1270, 1218, 1026, 934, 885, 775, 711; ^{1}H NMR (400 MHz, acetone-d_6) δ 8.48 (s, 1H), 8.35-8.30 (m, 1H), 7.74-7.68 (m, 1H), 7.46-7.42 (m, 1H), 7.36 (ddd, *J* 10.7, 8.4 and 1.2 Hz, 1H); ^{13}C NMR (100 MHz, acetone-d_6) δ 162.7, 162.2, 160.2, 145.5, 145.4, 135.4, 135.3, 132.2, 128.9, 125.1, 125.1, 120.0, 119.9, 116.3, 116.1, 115.0.

(*E*)-2-Cyano-3-(thiophen-2-yl)acrylic acid (**6l**)

$C_8H_5NSO_2$, 179.00 g mol^{-1}; 97% yield; brown crystal, mp 208-210 ºC; FTIR ν_{max} / cm^{-1} 3116, 2955, 2922, 2852, 2224, 1690, 1585, 1410, 1284, 1410, 1284, 1057, 944, 861, 740; ^{1}H NMR (500 MHz, DMSO-d_6) δ 8.53 (s, 1H), 8.16 (d, *J* 5.1 Hz, 1H), 8.00 (d, *J* 4.0 Hz, 1H), 7.33 (t, *J* 4.5 Hz, 1H); ^{13}C NMR (125 MHz, DMSO-d_6) δ 163.9, 147.4, 139.9, 136.8, 136.1, 129.1, 116.7, 99.7.

(*E*)-2-Cyano-3-(furan-2-yl)acrylic acid (**6m**)

$C_8H_5NO_3$, 163.03 g mol^{-1}; 99% yield; brown crystal, mp 168-170 ºC; FTIR ν_{max} / cm^{-1} 3433, 3186, 3091, 2998, 2924, 2230, 1700, 1605, 1589, 1492, 1412, 1261, 1201, 1185, 1092, 1014, 828, 789, 725; ^{1}H NMR (500 MHz, DMSO-d_6) δ 8.16 (d, *J* 1.7 Hz, 1H), 8.04 (s, 1H), 7.45 (d, *J* 3.7 Hz, 1H), 6.83 (dd, *J* 3.7 and 1.8 Hz, 1H); ^{13}C NMR (125 MHz, DMSO-d_6) δ 163.9, 150.0, 148.7, 139.0, 123.9, 116.3, 114.6, 99.1.

Results and Discussion

Cyanoacetic acid as a catalyst for Biginelli reaction

The first investigation of this study consisted of evaluating the ability of cyanoacetic acid to be a Bronsted acid-type organocatalyst for the Biginelli reaction. For this, the reaction using benzaldehyde **1a**, ethyl acetoacetate **2**, and urea **3** was evaluated as a protocol with different reactional conditions and the yields were calculated by

HPLC-DAD (Table 3).

The first experiment was performed in the absence of the catalyst and, with the reagents in the proportion of 0.5 mmol of aldehyde, 1 mmol of ethyl acetoacetate and, 0.75 mmol of urea. It was observed that in approximately 2 h of reaction, the agitation of the system was stopped due to precipitation of DHPM **4a**. Thus, 200 µL of EtOH were added to the reaction system, which regained its normal agitation. After 6 h of reaction, the DHPM **4a** was obtained in 55% yield (Table 3, entry 1).

In the following experiments, using this strategy of starting the reactions without solvent and adding the ethanol after 2 h, the catalytic effect of cyanoacetic acid on the Biginelli reaction was evaluated (Table 3, entries 2-7). In the first attempt, using 10 mol% of CA, and at 60 ºC, the DHPM **4a** was obtained in 66% yield with 4 h of reaction (Table 3, entry 2). Increasing the reaction time to 6 h, no significant changes were noted in the yield of **4a** (Table 3, entry 3). Varying the amount of CA to 20 mol%, it was observed that the yield increased to 80% for **4a** (Table 3, entry 4). Moreover, it was observed that when the temperature was changed to 80 ºC, the yield of DHPM **4a** was increased to 88% (Table 3, entry 5).

It was possible to realize that CA was acting as an organocatalyst in the reaction, since the reaction yields in its presence were higher than in the control experiment in the absence of catalyst. Also, it was observed that temperature was an important factor, and the best yield values were obtained at 80 ºC. Subsequently, a new test was performed in which the proportion of urea was decreased (0.5 mmol aldehyde, 1 mmol ethyl acetoacetate and 0.5 mmol urea). The result showed the same 88% yield for DHPM **4a** compared to the Table 3, entry 5 experiment, using a small amount of urea (Table 3, entry 6).

Finally, the optimized condition was tested in a microwave reactor (Table 3, entry 7); however, the yield under microwave irradiation was practically the same as that obtained through conventional heating conditions. Therefore, the conventional heating was then selected for the development of a scope of compounds.

For the development of the synthetic optimized protocol, several aromatic aldehydes were used, both with acceptor and electron donor groups linked in the aromatic ring. At the end of the process, DHPMs **4a**-**4h** were obtained with excellent yields 80-99% (Table 4) and characterized by NMR (^{1}H and ^{13}C), IR and melting point. It is noteworthy that the electronic effect of the aromatic ring substituents of the respective aldehydes did not influence the reactions and the yields of products, as well, although a significant amount of the CA was used, a gain of more than 30% in the reaction yield was observed, turning the catalytic role of cyanoacetic acid for the Biginelli reaction evident.

Figure 2 contains a proposed mechanistic route for the Biginelli reaction catalyzed by cyanoacetic acid (iminium route promoted by a Bronsted acid). The first step of the reaction includes the nucleophilic attack of the nitrogen from urea on the aldehyde, which was preliminary protonated by CA. In the sequence, after a dehydration, the iminium ion is formed. Following this route, the β-ketoester enolate attacked the iminium intermediate and CA was regenerated through a proton abstraction. In the final steps,

Table 3. Synthetic optimization process of DHPM **4a** using cyanoacetic acid as catalyst

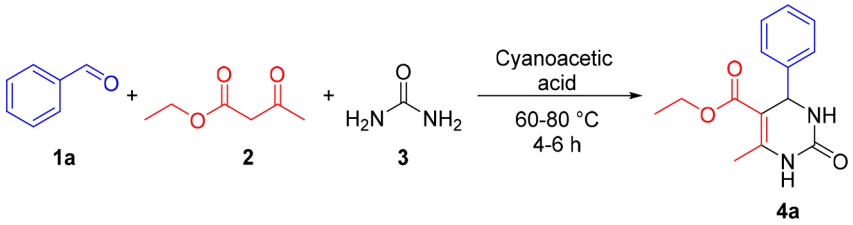

entry	Catalyst / mol%	Temperature / °C	time / h	Conversion / %
1	–	80	6	55
2	10	60	4	66
3	10	60	6	67
4	20	60	6	80
5	20	80	6	88
6	20	80	6	88[a]
7	20	80	6	86[a,b]

The reactions were performed initially for 2 h under free solvent. Then, 200 µL of EtOH were added and the reactions were performed in the appropriate time; reagents proportion: aldehyde (0.5 mmol), ethyl acetoacetate (1 mmol) and urea (0.75 mmol). [a]Proportion: aldehyde (0.5 mmol), ethyl acetoacetate (1 mmol) and urea (0.50 mmol); [b]Performed in MW reactor. Conversion determined by HPLC-DAD.

Table 4. Synthetic scope of DHPMs **4a**-**4h** using cyanoacetic acid as catalyst and conventional heating in the Biginelli reaction

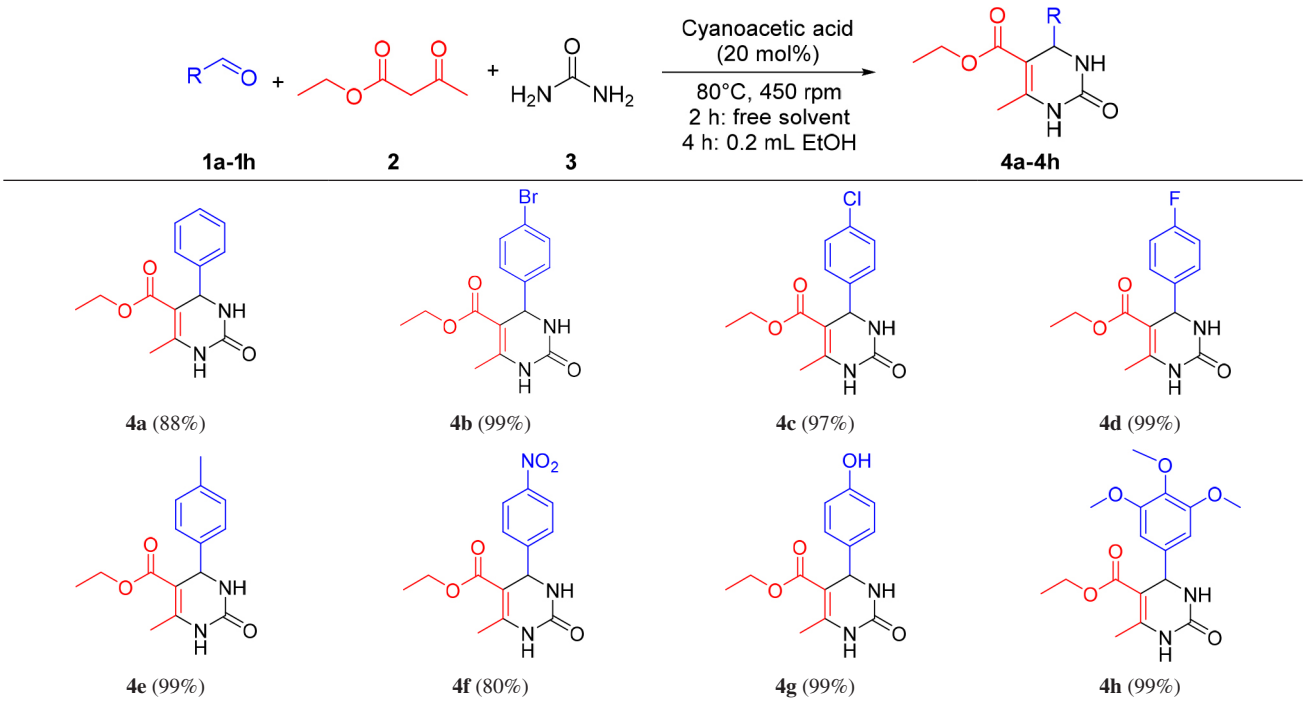

The reactions were performed initially for 2 h under free solvent. Then, 200 µL of EtOH were added and the reactions were performed for more 4 h. Reagents proportion: aldehyde (0.5 mmol), ethyl acetoacetate (1 mmol) and urea (0.50 mmol).

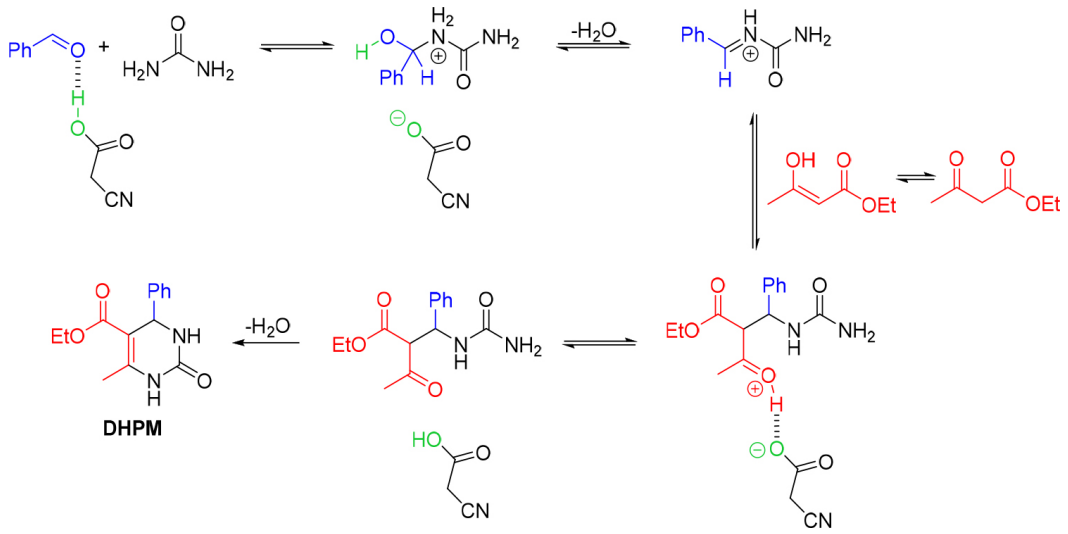

Figure 2. Proposed mechanism for the synthesis of DHPMs using cyanoacetic acid as catalyst.

an intramolecular cyclisation and another dehydration occurs, resulting in the DHPM structure.[33]

Cyanoacetic acid as a reagent for Knoevenagel condensation reaction

The reaction using furfural **1l** and CA **5** to produce the Knoevenagel adduct **6l** was selected for the optimization process involving different reaction conditions, using a MW reactor as heating source (Table 5). Initially, the experiment in absence of catalyst, for 20 min at 75 ºC did not produce compound **6l** (Table 5, entry 1). The use of a basic catalyst KOH (5 mol%, 0.7 M) was the first attempt to improve the reaction. In 20 min at 75 ºC, adduct **6l** was obtained with 51% yield (Table 5, entry 2). This experiment showed that the basic catalyst was essential for the formation of **6l**.

In the sequence, the temperature was kept constant at 75 ºC, the amount of KOH was increased to 10 mol% and

the yield of **6l** was increased to 71% (Table 5, entry 3). Increasing even more, using 20 mol%, adduct **6l** was obtained in 93% yield; however, no improvement in reaction yield was observed when 30 mol% of KOH was used (Table 5, entry 5).

The best condition achieved (Table 5, entry 4) was evaluated under conventional heating, to compare the effect of the heating source. The result was unsatisfactory and, adduct **6l** was obtained with only a 31% yield, showing the efficiency of the MW irradiation as a heating source for this protocol (Table 5, entry 6).

Furthermore, the possibility of a decrease in reaction time was investigated; however, when the reaction was performed in just 10 min, the adduct **6l** was obtained with 61% yield (Table 5, entry 8). In the last experiments, the effect of temperature was monitored. Through the results, it was possible to conclude that the temperature of 75 ºC had a direct influence on the yield of **6l**, since at lower temperatures the yield decreased significantly (Table 5, entries 9 and 10).

After the synthetic optimization process, a scope of molecules was obtained using CA as an activated methylene compound for the Knoevenagel condensation reaction with several aromatic aldehydes. As shown in Table 6, the Knoevenagel adducts **6a**-**6e** and **6h**-**6m** were obtained with good yields (65-97%), independently of the electronic characteristic of the substituent group attached to the aromatic ring.

Single crystals of **6a**, **6h**, **6l**, and **6m** suitable for X-ray diffraction analyses were obtained with the slow evaporation of solutions prepared for each compound using a mixture of acetone and methanol (1:1). The Oak Ridge Thermal Ellipsoid Plot (ORTEP) type representation of the crystal structures of these compounds are shown in Figure 3. Selected bond lengths and angles are available in the SI section.

The Knoevenagel adducts **6a**, **6h**, and **6l** crystallize in the triclinic space group P-1, while **6m** crystallizes in the monoclinic space group $P2_1/c$. As shown in Figure 3, the aromatic rings of adducts show high planarity, except **6h**, which possesses the carbon from the *p*-methoxy group positioned out of the plane of the aromatic ring. Furthermore, through these results, it was possible to observe the tendency of the formation of diastereoisomeric adducts with (*E*)-configuration.

The structures are stabilized by O–H···O hydrogen bonds, with these interactions giving rise to formation of dimeric arrangements. The non-classical hydrogen bonds such as C–H···O and C–H···N are also observed in the crystal packing of the adducts **6a**, **6h** and **6m**, and the combination of the non-covalent interactions present on these structures is helpful for the organization of the molecules of **6a** and **6h** in a one-dimensional chain, and **6m** in a two-dimensional network (see SI section).

Larvicidal activity for the synthesized Knoevenagel adducts

The Knoevenagel adducts **6a**-**6m** were tested for the 3rd instar larvae of *Aedes aegypti* (*A. aegypti*) at different concentrations (75, 50, 25, 15 and 7.5 μg mL^{-1}). The compounds **6c** and **6d** showed potential larvicidal activity, with a value of 100% mortality in 24 h, with LC_{50} and LC_{90} values of 19.63 and 33.84 μg mL^{-1} for compound **6c**, and

Table 5. Synthetic optimization process of Knoevenagel adduct **6l** using cyanoacetic acid and furfural under MW irradiation

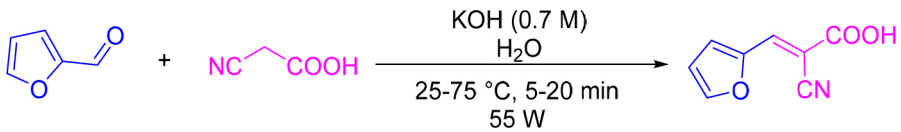

1l **5** **6l**

entry	Catalyst / %	Temperature / ºC	time / min	Isolated yield / %
1	–	75	20	0
2	KOH (5%, 0.7 M)	75	20	51
3	KOH (10%, 0.7 M)	75	20	71
4	KOH (20%, 0.7 M)	75	20	93
5	KOH (30%, 0.7 M)	75	20	95
6	KOH (20%, 0.7 M)	75	20	31[a]
7	KOH (20%, 0.7 M)	75	5	42
8	KOH (20%, 0.7 M)	75	10	61
9	KOH (20%, 0.7 M)	50	20	84
10	KOH (20%, 0.7 M)	25	20	69

Reagents proportion: aldehyde (1.0 mmol) and cyanoacetic acid (1.0 mmol). [a]Under conventional heating.

Table 6. Synthetic scope of Knoevenagel adducts **6a-6e**, **6h-6m** using cyanoacetic acid and aromatic aldehyde derivatives under MW irradiation

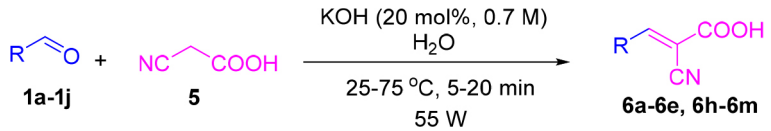

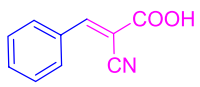 **6a** (71%)	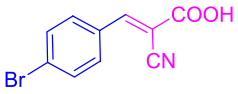 **6b** (82%)	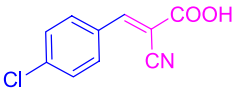 **6c** (85%)	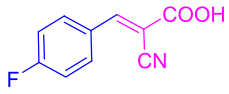 **6d** (75%)
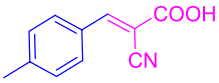 **6e** (83%)	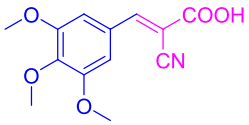 **6h** (78%)	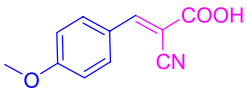 **6i** (65%)	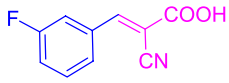 **6j** (68%)
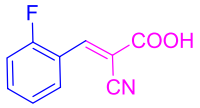 **6k** (65%)	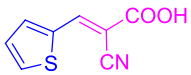 **6l** (97%)	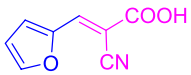 **6m** (92%)	

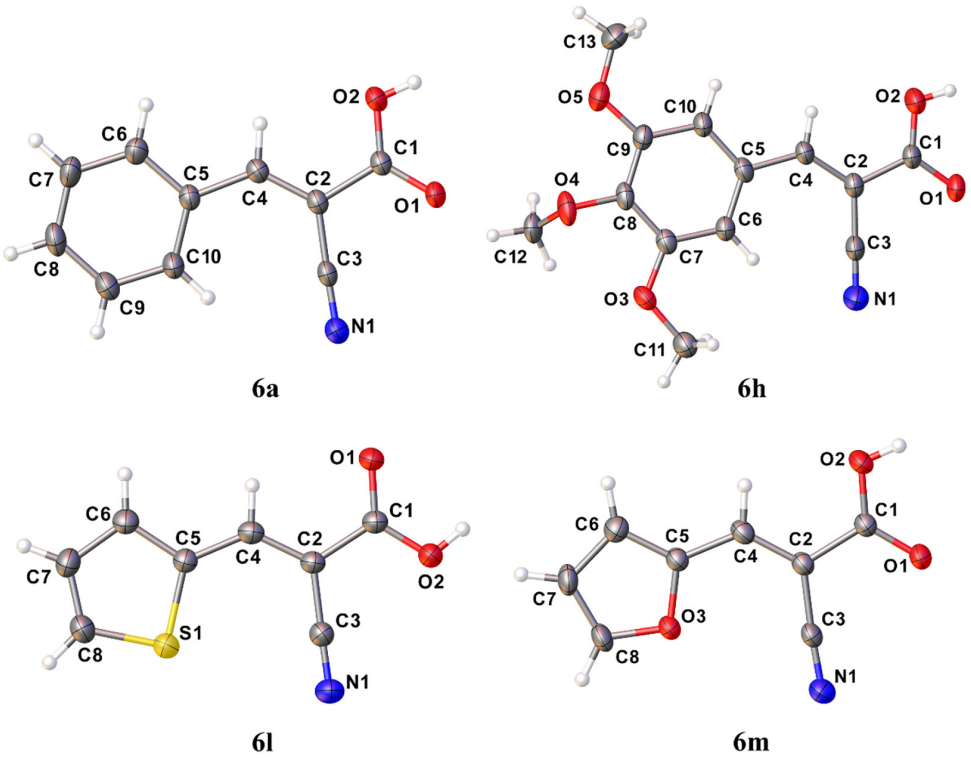

Figure 3. ORTEP type representation of the asymmetric units of compounds **6a**, **6h**, **6l** and **6m** showing 30% ellipsoids and labeling scheme.

27.46 and 48.16 μg mL^{-1} for compound **6d** (Table 7). The compounds **6b**-**6d** that showed potential larvicidal activity presented halogenated substituent groups attached in the aromatic ring (F, Cl, and Br).

Among the adducts **6a**, **6e**, **6h**, **6i**, **6l**, and **6m** (not halogenated), the compound **6a** showed larvicidal potential with LC_{50} values of 44.3 and 33.4 μg mL^{-1}. It also presented LC_{90} values of 90.9 and 76.6 μg mL^{-1} at 24 and 48 h, respectively (Table 8).

According to the study of Bianco *et al.*,[34] the stereoelectronic properties of compounds containing halogen substituents attached to the sesquiterpene showed

Table 7. Lethal concentration values (LC_{50} and LC_{90}) and confidence interval (CI) of compounds **6b**-**6d** with halogenated substituents attached in the aromatic ring

Compound	Values of LC_{50} and LC_{90} / (μg mL^{-1})			
	time (24 h)	CI	time (48 h)	CI
6b	78.7	(66.3-100.5)	64.8	(54.8-80.7)
6c	19.6	(17.3-22.4)	14.4	(12.3-16.7)
6d	27.4	(24.2-31.1)	14.9	(12.1-17.7)
	LC_{90} / (μg mL^{-1})			
	time (24 h)	CI	time (48 h)	CI
6b	140.8	(114.7-190.6)	127.2	(104.7-168.2)
6c	33.8	(29.6- 40.4)	27.8	(24.3-33.2)
6d	48.1	(42.7-55.8)	33.4	(28.9-40.6)

CI: confidence interval; LC: lethal concentration values.

larvicidal activities (> 91% at 50 ppm). When investigating larvicidal activity, the authors observed that molecules with electronegative substituent groups, e.g., chlorine and fluorine, influenced the solubility of the substance, the steric volume, and the interaction at the binding site.

The larvicidal results of some halogenated Knoevenagel adducts were tested for *A. aegypti* in the study by Carvalho *et al.*[35] Benzylidenemalononitriles, e.g., the (2-(4-chlorobenzylidene) malononitrile showed an effect against 3rd instar larvae showing LC_{50} values of 9.42 and 9.44 μg mL^{-1} at 24 and 48 h, respectively.

Aryl and phenoxymethyl-(thio)semicarbazones were also evaluated against *A. aegypti*. It was possible to observe the high activity of thiosemicarbazines, and the authors highlighted the importance of halogen substituent groups in the *para* position for this biological property. Atoms can interact through a halogen bond at the binding site of biological targets, and the presence of electron-donating groups may not present this desired activity.[36]

Finally, *A. aegypti* is an important vector for public health, and current strains show resistance to commercial insecticides. According to these results, the Knoevenagel compounds tested may be a promising alternative in the control of *A. aegypti*.

Larvicidal activity for the synthesized Biginelli compounds

The Biginelli compounds **4a**-**4h** were tested for the 3rd instar larvae of *Aedes aegypti* (*A. aegypti*) at different concentrations (75, 50, 25, 15 and 7.5 μg mL^{-1}), These

Table 8. Lethal concentration values (LC_{50} and LC_{90}) and confidence interval (CI) of compounds **6a**, **6e**, **6h**, **6i**, **6l**, without halogenated substituents attached in the aromatic ring

Compound	Values of LC_{50} and LC_{90} / (μg mL^{-1})			
	time (24 h)	CI	time (48 h)	CI
6a	44.3	(38.3-51.7)	33.4	(28.1-39.3)
6e	73.6	(62.8-91.5)	40.7	(35-47.4)
6h	58.4	(50.5-69.9)	38.3	(32.4-45.2)
6i	73.7	(60.9-96.8)	28.1	(21.9-34.7)
6l	81.5	(67.9-106.4)	37.2	(31.7-43.5)
6m	118.3	(88.8-203)	53.7	(46.6-63.3)
Compound	LC_{90} / (μg mL^{-1})			
	time (24 h)	CI	time (48 h)	CI
6a	90.9	(78.7-109.7)	76.8	(66.6-92)
6e	131.8	(109.1-172.9)	85.8	(74.5-03)
6h	112.2	(95-140.9)	86	(74.1-104.5)
6i	145.2	(115.9-204.3)	80	(67.7-100.1)
6l	147.1	(118.4-203.9)	82	(71.2-98.3)
6m	211.2	(151.8-389.4)	104	(89.1-128.1)

CI: confidence interval. LC: lethal concentration values.

compounds did not show any potential larvicidal activity with a value of 0% mortality in 24 and 48 h.

Validation of molecular docking protocols

Recovering the inhibitor pose (JHIII) was possible to validate the molecular docking protocols by superimposing the crystallographic pose over the best docking pose, obtaining a root-mean-square deviation (RMSD) value of 1.15 Å. According to Ramos *et al.*[37,38] the predicted binding mode in molecular docking indicates that when the RMSD ≤ 2.0 Å in relation to the crystallographic pose of a respective ligand, the validation is considered satisfactory (Figure 4).

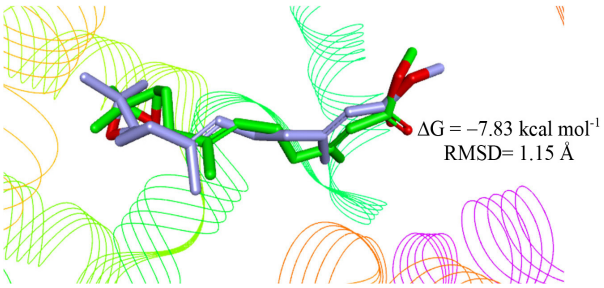

Figure 4. Overlay of crystallographic pose (blue) and molecular docking pose (green).

Interactions with the juvenile hormone protein binding site (PDB ID 5V13) are around the α-helix between amino acid residues 30-34, 45-51, 60-71, 123-130, 132-136 and 269 for the β-sheet between amino acid residues 52-55, 72-74 and 144-145. In the crystallographic ligand, it is possible to observe hydrophobic interactions with all amino acid residues in the binding site.

Evaluation of receptor-ligand interactions

Eleven compounds (Table 9) were subjected to molecular docking at the juvenile hormone (*Aedes aegypti*) binding site. In this study, only three adducts showed binding affinity values similar to or higher than the control used. Compound **6e** had a binding affinity of −8.0 kcal mol^{-1}, followed by **6j** with −8.0 kcal mol^{-1} and **6k** with −8.1 kcal mol^{-1} compared to the control (JHIII).

Individual interactions observed in the docking of compounds **6e**, **6j**, and **6k** were similar to those observed for JHIII in the juvenile hormone-binding site, around the α-helix between the amino acid residues Trp33-Val-65 and in the β-sheet with Val-51, Trp-53, and Pro-55, as shown in Figure 5.

A single well-ordered molecule of JHIII (refined occupations 0.91-0.96) is present in the binding pocket of

Table 9. Results of binding affinity of the compounds **6a**-**6m** with the juvenile hormone protein

Complex	Binding affinity / (kcal mol^{-1})
JHIII	–8.4
6a	–7.6
6b	–7.8
6c	–7.8
6d	–7.9
6e	–8.0
6h	–7.1
6i	–7.8
6j	–8.0
6k	–8.1
6l	–6.6
6m	–6.6

the *N*-terminal domain of mJHB. According to Kim *et al.*,[39] three molecules of the complex are present in the asymmetric unit of the crystal, and the ligand conformation is essentially identical in all three. The JHIII epoxy is located in the center of the domain, while the methyl ester group of the hormone is oriented towards its surface. The epoxy group forms a hydrogen bond with the phenolic hydroxyl of Tyr-129, and the remainder of the isoprenoid chain is surrounded by hydrophobic side chains including those of Phe-144, Tyr-64, Trp-53, Val-65, Val -68, Leu-72, Leu-74, Val-51 and Tyr-33.

Compound **6k** presented significant contributions to the binding affinities (–8.1 kcal mol^{-1}), as the study complies with the pocket binding site, in which they are represented by amino acids surrounded by hydrophobic side chains including Try-33, and Trp-53, and a hydrogen bond with Val-51.

Conclusions

The use and application of CA were evaluated in two distinct roles, as a catalyst and as a reagent for the synthesis of organic compounds. According to experimental results, CA had catalytic activity, improving the Biginelli reaction. Through its use as an organocatalyst, it was possible to synthesize eight DHPMs **4a**-**4h** in good yields of 80-99% using ethanol as a green solvent. Furthermore, the use of CA as a reagent for the Knoevenagel condensation reaction was explored. Using KOH as a base catalyst, it was possible to obtain eleven examples of adducts in the (*E*)-configuration with good yields of 65-97%, using water as a green solvent under microwave irradiation.

The larvicide studies showed that Knoevenagel adducts, containing halogenated substituent groups

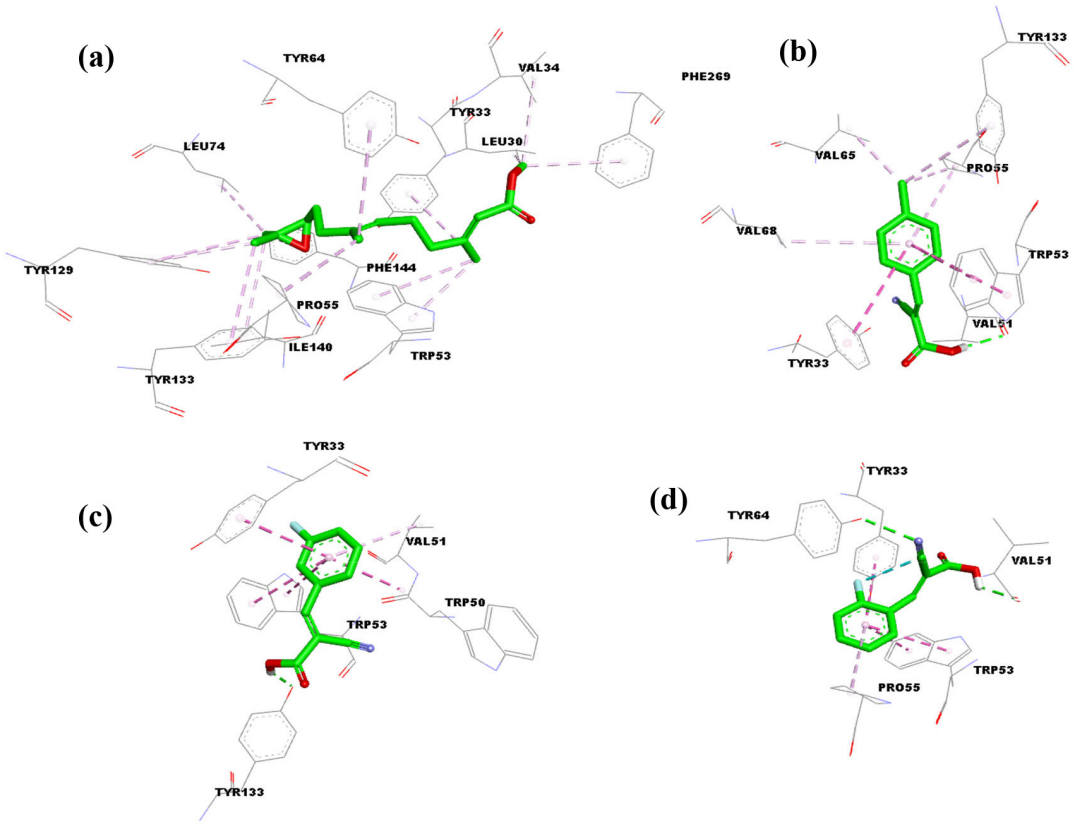

Figure 5. Mode of binding of molecules with major interaction in the juvenile hormone receptor: (a) JHIII, (b) **6e**, (c) **6j** and (d) **6k**.

attached in the aromatic ring have potential larvicidal activity with 100% mortality in 24 h with LC_{50} and LC_{90} for values of 19.63 and 33.84 μg mL^{-1} and, 27.46 and 48.16 μg mL^{-1}, respectively.

Therefore, CA is a promising stable compound with low cost that can be used as a catalyst and a reagent in organic chemistry. Moreover, the products obtained by its use are easily purified and can be used as larvicide control against *Aedes aegypti*.

Supplementary Information

The Crystallographic Information File (CIF) of Knoevenagel adduct derivatives **6a**, **6h**, **6l** and **6m** were deposited in the Cambridge Structural Data Base under the Cambridge Crystallographic Data Centre (CCDC) numbers 2298597, 2298598, 2298599 and 2298600, respectively. Copies of the data can be obtained, free of charge, via www.ccdc.cam.ac.uk.

Supplementary information is available free of charge at http://jbcs.sbq.org.br as PDF file.

Acknowledgments

L. L. Zanin thanks for the scholarships financed by the Coordenação de Aperfeiçoamento de Pessoal de Nível Superior - Brazil (CAPES) - Finance Code 001. This study was also funded by Fundação de Amparo à Pesquisa do Estado de São Paulo (FAPESP) projects 2019-07654-2/2016-20155-7 and Conselho Nacional de Desenvolvimento Científico e Tecnológico (CNPq) projects 302528/2017-2 and 303355/2021-2. The authors are grateful to the Brazilian funding agencies FAPESP (2017/15840-0 and 2021/10066-5), CNPq (312505/2021-3).

Author Contributions

Lucas L. Zanin was responsible for conceptualization, methodology, formal analysis, data curation, writing (original draft, review and editing of the manuscript); David E. Q. Jimenez for conceptualization, methodology, formal analysis, data curation, writing (original draft, review and editing of the manuscript); Gabriel S. Baia for the conceptualization, methodology, formal analysis, data curation, writing (original draft, review and editing of the manuscript); Victor Hugo Marinho for the methodology of the manuscript; Inana F. de Araujo for the conceptualization, methodology, formal analysis, data curation, writing (original draft, review and editing of the manuscript); Ryan S. Ramos for the conceptualization, methodology, formal analysis, data curation, writing (original draft, review and editing of the manuscript); Raimundo N. Soto for the methodology of the

manuscript; Irlon M. Ferreira for the methodology of the manuscript; Pedro Henrique O. Santiago for the methodology, formal analysis, data curation, writing (original draft, review and editing of the manuscript); Javier A. Ellena for the project administration and the funding acquisition of the manuscript; André Luiz M. Porto for the conceptualization, project administration and the funding acquisition of the manuscript.

References

1. Singh, K.; Singh, K.; Wan, B.; Franzblau, S.; Chibale, K.; Balzarini, J.; *Eur. J. Med. Chem.* **2011**, *46*, 2290. [Crossref]
2. Insuasty, D.; Castillo, J.; Becerra, D.; Rojas, H.; Abonia, R.; *Molecules* **2020**, *25*, 505. [Crossref]
3. Mayer, T. U.; Kapoor, T. M.; Haggarty, S. J.; King, R. W.; Schreiber, L.; Mitchison, T. J.; *Science* **1999**, *286*, 971. [Crossref]
4. Chikhale, R. V.; Bhole, R. P.; Khedekar, P. B.; Bhusari, K. P.; *Eur. J. Med. Chem.* **2009**, *44*, 3645. [Crossref]
5. da Silva, D. L.; Reis, F. S.; Muniz, D. R.; Ruiz, A. L. T.; de Carvalho, J. E.; Sabino, A. A.; Modolo, L. V.; de Fátima, Â.; *Bioorg. Med. Chem.* **2012**, *20*, 2645. [Crossref]
6. Ramajayam, R.; Tan, K.-P.; Liu, H.-G.; Liang, P.-H.; *Bioorg. Med. Chem. Lett.* **2010**, *20*, 3569. [Crossref]
7. Lewis, R. W.; Mabry, J.; Polisar, J. G.; Eagen, K. P.; Ganem, B.; Hess, G. P.; *Biochemistry* **2010**, *49*, 4841. [Crossref]
8. Crnogorac, M. Đ.; Matić, I. Z.; Damjanović, A.; Janković, N.; Krivokuća, A.; Stanojković, T.; *Chem. Biol. Interact.* **2021**, *345*, 109565. [Crossref]
9. Attri, P.; Bhatia, R.; Gaur, J.; Arora, B.; Gupta, A.; Kumar, N.; Choi, E, H.; *Arabian J. Chem.* **2017**, *10*, 206. [Crossref]
10. Kwon, O. W.; Moon, E.; Chari, M. A.; Kim, T. W.; Kim, A. J.; Lee, P.; Ahn, K. H.; Kim, S. Y.; *Bioorg. Med. Chem. Lett.* **2012**, *22*, 5199. [Crossref]
11. Zhao, Y.; Wu, H.; Wang, Z.; Wei, Y.; Wang, Z.; Tao, L.; *Sci. China: Chem.* **2016**, *59*, 1541. [Crossref]
12. Zhu, Y. C.; Yang, B.; Zhao, Y.; Fu, C.; Tao, L.; Yen, W.; *Polym. Chem.* **2013**, *4*, 5395. [Crossref]
13. Ma, Z.; Wang, B.; Tao, L.; *Molecules* **2022**, *27*, 7886. [Crossref]
14. Mao, T.; He, X.; Liu, G.; Wei, Y.; Gou, Y.; Zhou, X.; Tao, L.; *Polym. Chem.* **2021**, *12*, 852. [Crossref]
15. Gilanizadeh, M.; Zeynizadeh, B.; *Res. Chem. Intermed.* **2018**, *44*, 6053. [Crossref]
16. Zanin, L. L.; Porto, A. L. M.; *ChemistrySelect* **2020**, *5*, 8604. [Crossref]
17. Jimenez, D. E. Q.; Zanin, L. L.; Diniz, L. F.; Ellena, J.; Porto, A. L. M.; *Curr. Microwave Chem.* **2019**, *6*, 54. [Crossref]
18. *CrysAlisPRO*, version 1.171.37.33; Agilent Technologies UK Ltd, Yarnton, UK, 2014.
19. Dolomanov, O. V.; Bourhis, L. J.; Gildea, R. J.; Howard, J. A. K.; Puschmann, H.; *J. Appl. Crystallogr.* **2009**, *42*, 339. [Crossref]
20. Sheldrick, G. M.; *Acta Crystallogr. Sect. A: Found. Crystallogr.* **2015**, *A71*, 3. [Crossref]
21. Sheldrick, G. M.; *Acta Crystallogr. Sect. C: Struct. Chem.* **2015**, *C71*, 3. [Crossref]
22. Groom, C. R.; Bruno, I. J.; Lightfoot, M. P.; Ward, S. C.; *Acta Crystallogr. Sect. B: Struct. Sci., Cryst. Eng. Mater.* **2016**, *72*, 171. [Crossref]
23. World Health Organization (WHO); *Guidelines for Laboratory and Field Testing of Mosquito Larvicides*; Communicable Disease Control, Prevention and Eradication, WHO Pesticide Evaluation Scheme: Geneva, Switzerland, 2005. [Link] accessed in December 2023
24. de Araújo, I. F.; de Araújo, P. H. F.; Ferreira, R. M. A.; Sena, I. D. S.; Lima, A. L.; Carvalho, J. C. T.; Ferreira, I. M.; Souto, R. N. P.; *S. Afr. J. Bot.* **2018**, *117*, 134. [Crossref]
25. *Minitab*, version 21.4.0; Minitab Statistical Software; State College, Pennsylvania, USA, 2023.
26. Lee, C.; Yang, W.; Parr, R. G.; *Phys. Rev. B* **1988**, *15*, 785. [Crossref]
27. Palheta, I. C.; Ferreira, L. R.; Vale, J. K. L.; Silva, O. P. P.; Herculano, A. M.; Oliveira, K. R. H. M.; Chaves Neto, A. M. J.; Campos, J. M.; Santos, C. B. R.; Borges, R. S.; *Molecules* **2020**, *25*, 3330. [Crossref]
28. Frisch, M. J.; Trucks, G. W.; Schlegel, H. B.; Scuseria, G. E.; Robb, M. A.; Cheeseman, J. R.; Scalmani, G.; Barone, V.; Mennucci, B.; Petersson, G. A.; Nakatsuji, H.; Caricato, M.; Li, X.; Hratchian, H. P.; Izmaylov, A. F.; Bloino, J.; Zheng, G.; Sonnenberg, J. L.; Hada, M.; Ehara, M.; Toyota, K.; Fukuda, R.; Hasegawa, J.; Ishida, M.; Nakajima, T.; Honda, Y.; Kitao, O.; Nakai, H.; Vreven, T.; Montgomery Jr., J. A.; Peralta, J. E.; Ogliaro, F.; Bearpark, M.; Heyd, J. J.; Brothers, E.; Kudin, K. N.; Staroverov, V. N.; Kobayashi, R.; Normand, J.; Raghavachari, K.; Rendell, A.; Burant, J. C.; Iyengar, S. S.; Tomasi, J.; Cossi, M.; Rega, N.; Millam, N. J.; Klene, M.; Knox, J. E.; Cross, J. B.; Bakken, V.; Adamo, C.; Jaramillo, J.; Gomperts, R.; Stratmann, R. E.; Yazyev, O.; Austin, A. J.; Cammi, R.; Pomelli, C.; Ochterski, J. W.; Martin, R. L.; Morokuma, K.; Zakrzewski, V. G.; Voth, G. A.; Salvador, P.; Dannenberg, J. J.; Dapprich, S.; Daniels, A. D.; Farkas, Ö.; Foresman, J. B.; Ortiz, J. V.; Cioslowski, J.; Fox, D. J.; *Gaussian-09*, Revision D.01; Gaussian, Inc., Wallingford CT, 2009.
29. *Discovery Studio*, 5.0; Dassault Systemes BIOVIA, San Diego, California, USA, 2009.
30. *AutoDock*, 4.2.; Center for Computational Structural Biology, La Jolla, California, USA, 2022.
31. *AutoDockVina*, 1.1.2.; Center for Computational Structural Biology; La Jolla, California, USA, 2022.
32. PyRx, https://pyrx.sourceforge.io, accessed in December 2023.
33. de Souza, R. O. M. A.; da Penha, E. T.; Milagre, H. M. S.; Garden, S. J.; Esteves, P. M.; Eberlin, M. N.; Antunes, O. A.

C.; *Chem. - Eur. J.* **2009**, *15*, 9799. [Crossref]
34. Bianco, E. M.; Pires, L.; Santos, G. K. N.; Dutra, K. A.; Reis, T. N. V.; Vasconcelos, E. R. T. P. P.; Cocentino, A. L. M.; Navarro, D. M. A. F.; *Ind. Crops Prod*. **2013**, *43*, 270. [Crossref]
35. Carvalho, H. L.; Amorim, A.; Araujo, L. L. F.; Marino, B. L. B.; Jimenez, D. E. Q.; Ferreira, R. M. A.; Hage-Melim, L. I. P.; Souto, R. N. S.; Porto, A. L. M.; *Rev. Virtual Quim*. **2018**, *10*, 362. [Crossref]
36. da Silva, J. B.; Navarro, D. M.; da Silva. A. G.; Santos, G. K.; Dutra, K. A.; Moreira, D. R.; Ramos, M. N.; Espíndola, J. W.; de Oliveira, A. D.; Brondani, D. J.; Leite, A, C.; Hernandes, M. Z.; da Rocha, V. R.; de Castro, F. M. C.; de Oliveira, B. C.; Lan, Q.; Pereira, K. M.; *Eur. J. Med. Chem*. **2015**, *100*, 162. [Crossref]
37. Ramos, R. S.; Costa, J. S.; Silva, R. C.; da Costa, G. V.; Rodrigues, A. B. L.; Rabelo, É. M.; Souto, R. N. P.; Taft, C. A.; da Silva, C. H. T. P.; Rosa, J. M. C.; dos Santos, C. B. R.; Macedo, W. J. D.; *Pharmaceuticals* **2019**, *12*, 20. [Crossref]
38. Ramos, R. S.; Macêdo, W. J. C.; Costa, J. S.; da Silva, C. H. T. P.; Rosa, J. M. C.; da Cruz, J. N.; de Oliveira, M. S.; Aguiar, A. E. H.; de Silva, R. B. L.; Souto, R. N. P.; Santos, C. B. R.; *J. Biomol. Struct. Dyn.* **2020**, *38*, 4687. [Crossref]
39. Kim, I. H.; Pham, V.; Jablonka, W.; Goodman, W. G.; Ribeiro, J. M. C.; Andersen, J. F.; *J. Biol. Chem.* **2017**, *292*, 15329. [Crossref]

Submitted: October 3, 2023
Published online: January 10, 2024